Pure & Appl. Chem., Vol. 62, No. 5, pp. 815–824, 1990.
Printed in Great Britain.

The role of ions in soot formation

H. F. Calcote and D. G. Keil

AeroChem Research Laboratories, Inc., P.O. Box 12, Princeton, NJ, 08542, USA

Abstract - The ionic mechanism of soot formation assumes rapid growth of ions from the chemiion $C_3H_3^+$ to form increasingly larger ions which either become incipient charged soot particles or combine with electrons (produced in the chemiionization step) to produce incipient neutral soot particles. A comparison of the rates of total ion formation with the rates of soot formation demonstrates that the rate of ion formation exceeds the rate of soot formation, and that the rate at which ions disappear is approximately equal to the rate at which soot is formed. In addition, ions are observed to disappear at the same point in the flame at which soot is observed to form. The time it takes to add 10 carbon atoms, i.e., to grow from C_{10} to C_{20} species, is compared for the neutral and ionic mechanisms. These times, using experimentally measured species concentrations and typical rate coefficients, are comparable for the two mechanisms. The higher concentrations of neutral species are balanced by the greater reaction rate coefficients for ion-molecule reactions, and by the fewer number of steps involved in adding a specific number of carbon atoms for the ionic mechanism than for the neutral mechanism.

INTRODUCTION

There are essentially two current mechanisms proposed for soot formation in flames. The more generally accepted mechanism involves neutral free radicals and is represented by the mechanism proposed by Frenklach and associates (ref. 1, 2). The other mechanism involves ions and has been championed by Calcote and associates (ref. 3-5). We recently summarized some of the evidence in support of the ionic mechanism (ref. 6). Here we review the tenets of the ionic mechanism, compare the rate of ion formation with the rate of soot formation, and compare the rate of adding carbon atoms to a molecular system by the two mechanisms.

IONIC MECHANISM OF SOOT FORMATION

The ionic mechanism is placed in the context of the total mechanism of soot formation in Fig. 1. The ionic mechanism starts with the chemiion, $C_3H_3^+$, which rapidly grows by the addition of acetylene, or other small neutral species. As an ion becomes larger, its electron recombination coefficient increases and it is more likely to be removed from the system by recombination with the electrons produced in the initial chemiionization process. The growing ions either become charged soot particles or following recombination with electrons (produced in the chemiionization step) yield neutral species which can continue to grow, as in the neutral mechanism, to become neutral particles. These particles, neutral or charged, continue to grow by the addition of acetylene. In a hot flame, or one in which alkali metals have been added to produce ions, the particles can become charged by thermal ionization or by diffusive charging. The charge on the particle can play an important role in determining the rate of coagulation. The latter stages of soot particle growth, by acetylene addition reactions and by coagulation are common to both the neutral free radical mechanism and to the ionic mechanism. The differences between the two mechanisms are in the details of the

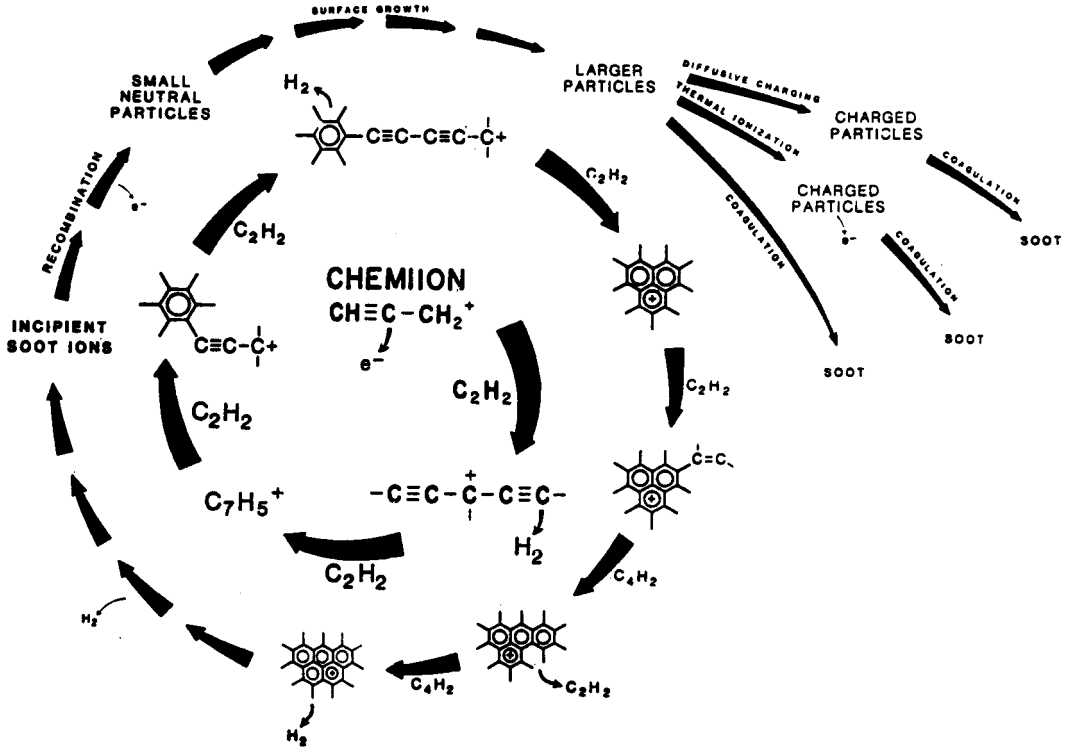

Fig. 1. Chemiions to soot.

mechanism of nucleation, i.e., in the initial reactions by which the chemical species change from small molecules to very large molecules, i.e., from a system characterized as chemical, in which chemical kinetics dominates, to one characterized as particulate, in which particle dynamics dominates.

The ionic mechanism assumes the precursor of soot formation to be $C_3H_3^+$, the dominant ion in fuel rich hydrocarbon flames. The source of this ion is (ref. 3, 7):

$$CH^* + O \rightarrow CHO^+ + e^- \quad (1)$$

followed by several reaction paths to produce $C_3H_3^+$, e.g.:

$$CHO^+ + CH_2 \rightarrow CH_3^+ + CO \quad (2)$$

$$CH_3^+ + C_2H_2 \rightarrow C_3H_3^+ + H_2 \quad (3)$$

and

$$CHO^+ + H_2O \rightarrow H_3O^+ + CO \quad (4)$$

$$H_3O^+ + C_3H_2 \rightarrow C_3H_3^+ + H_2O \quad (5)$$

There are two isomeric structures of $C_3H_3^+$, a stable cyclic structure, cyclopropenyl, and a linear structure, propargyl. Measurements near room temperature demonstrate that reactions of propargyl are fast, $k = 1 \times 10^{-9}$ cm^3 s^{-1}, generally equal to the Langevin rate, while the rate coefficients for comparable cyclopropenyl reactions are much smaller (ref. 8, 9). Eyler and associates (ref. 10) found the condensation reaction of propargyl with C_2H_2 to be slow, $k < 5 \times 10^{-12}$ cm^3 s^{-1}, although they confirmed that its reaction with C_4H_2 to produce C_5H_x is fast, $k = 1.4 \times 10^{-9}$ cm^3 s^{-1}. In contrast, at a higher pressure (40-100 Pa), Smith and Adams (ref. 11) observed rapid reaction of C_2H_2 with both propargyl, $k = 1.1 \times 10^{-9}$ cm^2 s^{-1}, and cyclopropenyl, $k \leq 1 \times 10^{-11}$ cm^3 s^{-1}. Thus the value of the rate coefficient for the reaction of the propargyl ion with acetylene appears unsettled.

The above rate coefficients were measured near room temperature and the validity of extrapolating them to high temperatures is not clear. Langevin theory (ref. 12), which does not predict a temperature dependence for ions reacting with non-polar molecules, has been well tested at ambient temperatures and is generally consistent with experiments (ref. 8, 9, 11). However, Langevin theory accounts only for the rate of production of an ion-molecule complex and not the fate of the nascent complex; thus at higher temperatures the dissociation paths may differ from those at room temperature. We have presented evidence that ion-molecule reactions are rapid at flame temperatures (ref. 5), but ion-molecule rate coefficients need to be measured at flame temperatures.

Which isomer of $C_3H_3^+$ is formed in Reactions such as (3) and (5) is also unknown. These reactions are exothermic for producing either isomer: 100-150 kJ/mol for propargyl and 200-250 kJ/mol for cyclopropenyl. At flame temperatures the two isomers should be in equilibrium (ref. 13). Accurate data on which isomer is produced in the flame and the rate of isomerization are clearly important to quantitative tests of the ionic mechanism of soot formation.

The ionic mechanism posits that the precursor ions react with neutral species, e.g., acetylenes to produce larger ions, e.g.:

$$C_3H_3^+ + C_2H_2 \rightarrow C_5H_3^+ + H_2 \quad (6)$$

$$C_3H_3^+ + C_4H_2 \rightarrow C_7H_5^+ \quad (7)$$

These ions sequentially and rapidly add low molecular weight neutral species, e.g., acetylenes, to produce increasingly larger ions (ref. 5, 6). All of the individual ions involved in the postulated mechanism, up to mass 557, have been observed in sooting flames (ref. 4, 5, 14).

Some electrons produced in Reaction (1) produce negative ions by attaching to large molecules; these reactions are favored by low temperature and increasing molecular weight. Ion-electron recombination rate coefficients are about 2×10^{-7} cm^3 s^{-1} for small ions at flame temperatures, and are about two orders of magnitude smaller for ion-ion recombination. The ion-electron recombination rate coefficients increase with increasing molecular weight so that as ions grow larger, positive ions are recombined more rapidly to form neutral incipient soot particles or precursors of neutral species.

SOME EXPERIMENTAL OBSERVATIONS

Ion concentrations in premixed sooting flames have been measured at AeroChem (ref. 4, 5) and by Delfau and associates (ref. 14) in a sooting (ϕ = 3.0), acetylene/oxygen flame on a flat flame burner at 2.7 kPa and unburned gas velocity of 50 cm s^{-1}. Temperature profiles, neutral species concentration profiles, and the concentration profiles of both neutral and charged soot particles have also been measured on an identical burner under essentially the same conditions (ref. 15-17). This flame is thus completely characterized and serves as a standard for examining mechanisms. Some of the individual species profiles for this flame are presented in Fig. 2. The temperature, total ion concentration, and the neutral and charged soot particle concentration profiles are presented in Fig. 3. Identifiable soot particles, (i.e., those which can be detected using an electron microscope, diameter exceeding about 1.5 nm) first appear at about 2.0 cm above the burner, yet a yellow glow, presumably due to soot, first appears at about 1.0 cm. To reflect this observation--i.e., that soot is formed where the yellow glow appears even though the particles are too small to be detected with the electron microscope--we have drawn, in Fig. 3, an interpolated (dotted) soot concentration curve starting at 1 cm and extending to the measured maximum.

Several immediate observations are apparent on inspection of Fig. 2 relative to the mechanism of soot formation. The most obvious is that neutral species concentrations are orders of

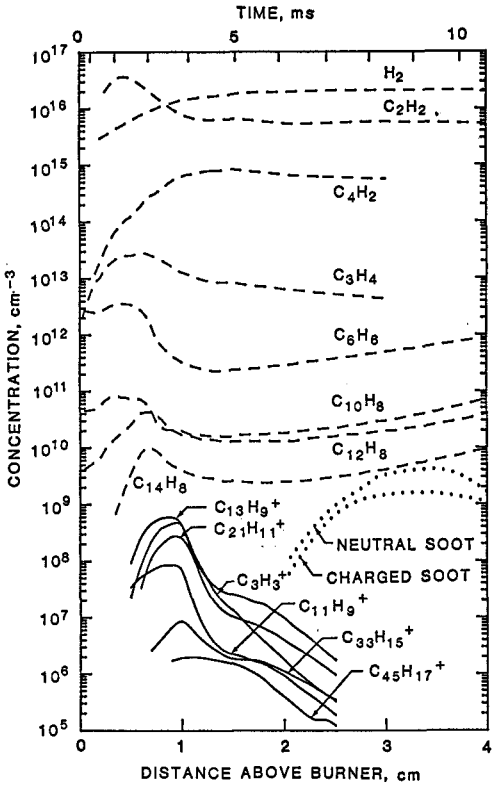

Fig. 2. Selected profiles in the standard C_2H_2/O_2 flame.

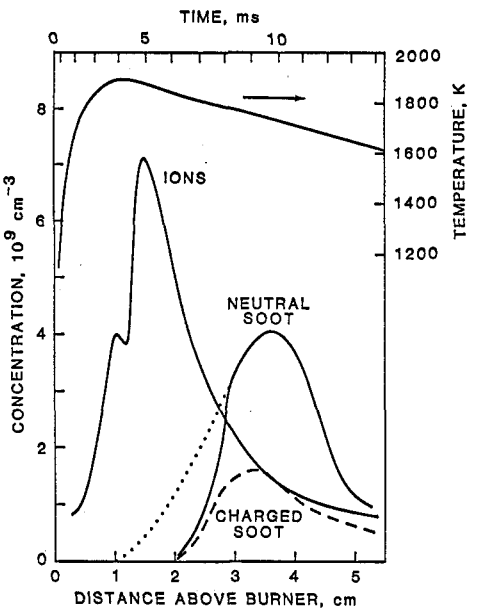

Fig. 3. Comparison of total ion concentration and soot concentration profiles in the standard acetylene/oxygen flame. The dotted curve is an interpolation of the NEUTRAL SOOT profile to give a finite value at the first observation of yellow emission near 1 cm. See text.

magnitude greater than ion concentrations; this has led to the general bias favoring neutral mechanisms of soot formation over ionic mechanisms. On further inspection it is noted that the concentrations of the larger observed neutral species approach the ion concentrations, and that many of the observed ion masses are much higher than those of the neutrals. Another relevant observation is that the ion concentrations decay at just the point in the flame that soot is observed to increase. There is thus an apparent connection between the disappearance of ions and the formation of soot. On the other hand, there seems to be no such obvious correlation between a decay in neutrals and the formation of soot. In fact, neutral PCAH concentrations are still increasing after the peak in soot concentration is reached. With respect to reactants available as building blocks, it is clear that acetylene and diacetylene are the only candidates, and unless diacetylene reactions have rate coefficients about an order of magnitude greater than acetylene reactions, acetylene is the only major building block. Clearly reactions among most of the species can not be fast enough, because of the low concentrations, to play a major role. Thus, building ions from reactions such as:

$$C_3H_3^+ + C_{10}H_8 \rightarrow C_{13}H_{11}^+ \quad (8)$$

$$\rightarrow C_{13}H_9^+ + H_2 \quad (9)$$

must be ruled out of consideration.

RATES OF ION FORMATION

One requirement of any mechanism of soot formation is that the rate of formation of soot precursors equal or exceed the rate at which soot is produced. In this section we examine the experimental data in Fig. 4 to compare the experimental rate at which the total number of ions is generated with the rate at which neutral soot is observed to be formed.

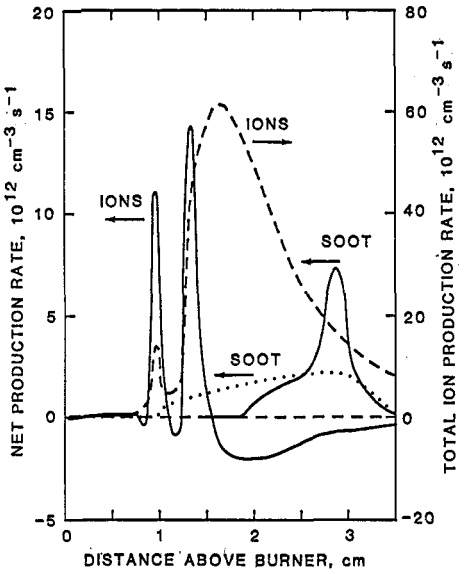

Fig. 4. Production rates of ions and soot in Fig. 3 flame. Net production rates of ion and soot based on concentration profiles, Fig. 3, with solid and dotted neutral SOOT curves corresponding in both figures. Dashed curve (note different scale) is the total ion production rate. See text.

Treating the flame as a steady state, one-dimensional system, and neglecting thermal diffusion, the continuity equation describing the ion concentration at any distance from the burner is:

$$(dI/dt) = (\text{net ion production rate}) - V(dI/dx) + D(d^2I/dx^2) = 0 \qquad (1)$$

where I = ion concentration, V = flow velocity, D = ion diffusion coefficient, and x is the distance from the burner. V has been determined as a function of distance in this flame (ref. 4), and D was calculated from estimated ion mobilities, μ (ref. 4), using the Einstein relation: $D = \mu(kT/e)$, where k is the Boltzman constant and e the electronic charge. Combining these values with the ion concentration derivatives of the profile in Fig. 3 gives the "net ion production rate" as shown in Fig. 4.

The total ion production rate, q, was obtained by adding the calculated ion loss rate by recombination with free electrons, to the "net ion production rate". The ion recombination rate is αI^2, where α is the ion-electron recombination coefficient. For α we used 2×10^{-7} cm^3 s^{-1} where small (i.e., 39 amu) ions dominate, and corrected for increasing ion mass downstream in the flame (ref. 4) using a factor proportional to d^2 where d = ion diameter and a capacitive term of the form (1 + A/d) with A a constant. The total ion production rate, q, is also plotted in Fig. 4 as a dashed line--note scale change. If negative ions are assumed to be the recombining partners for positive ions, the total ion production rates would be reduced because ion-ion recombination is slower than ion-electron recombination.

The net ion production rate shows two peaks corresponding to the two peaks in the ion concentration curve; the source of these two peaks is unknown. Also shown in Fig. 4 is the net rate of particle formation derived from the two neutral soot curves in Fig. 3 using Eq. (1), in which the diffusion term is now negligible compared with the flow velocity term for these large particles.

The first observation is that the maximum net rate of ion formation, 1.5×10^{13} ions cm^{-3} s^{-1}, exceeds the net rates of soot formation, 2.5 and 7.5×10^{12} particles cm^{-3} s^{-1} from either curve. Second, the net ion loss and soot formation occur in the same region of the flame. Third, the net ion loss rate, about 2×10^{12} cm^{-3} s^{-1}, corresponds with the net particle formation rate, about 2×10^{12} cm^{-3} s^{-1} assuming particles first appear at the position in the flame where yellow first occurs (dotted curve, Figs. 3 and 4). The peak particle production rate for the measured soot curve is only about four times greater than the peak ion net loss rate. The value for the net ion disappearance rate, however, does

not include larger ions lost by recombination which can still lead to soot formation via the same types of reactions as in the postulated free radical mechanisms.

These analyses lend further support to an ionic mechanism of soot formation in this flame. Clearly more precise data are desirable, particularly on negative molecular ions and on their rates of recombination, and particle concentration and particle size distribution (both neutral and charged) where soot is first observed, i.e., where the yellow emission first appears.

COMPARISON OF NEUTRAL AND IONIC MECHANISMS

The objective of the following analysis is to compare the rate of formation of large carbon species, which presumably lead to soot, by the neutral free radical mechanism and by the ionic mechanism. We do this by following a specific number of growing molecular species, neutral or ion, through a series of growth steps, and compare the time required by the two competitive mechanisms to add a specific number of carbon atoms. Experimentally measured concentrations of both neutral and ionic species in the standard acetylene flame (ref. 6), some shown in Fig. 2, are used in the comparison. This automatically takes care of all complications due to side reactions (formation and destruction), and diffusion of the specific species, and thus simplifies the argument. These experimental concentrations are combined with the rate coefficients for the growth of that species to the next larger species in the reaction sequence, and a time is calculated for each step in adding carbon atoms. The times for the species to add a specified number of carbon atoms by the two mechanisms are then compared.

Thus, for the general reaction:

$$A + B \rightarrow C + D \tag{10}$$

the rate of reaction is given by:

$$R = \frac{dC}{dt} = kAB \tag{2}$$

here A, B, and C represent the concentrations of the respective reactants and products. For this analysis we use the maximum experimental concentrations of A (with respect to distance from the burner), and use the measured value of B at the position in the flame where the concentration of A is maximum, i.e., we consistently compute the maximum rate of conversion of A and B to C and D. The appropriate rate coefficient, k, is used for either the free radical or the ionic mechanism. In the free radical mechanism (ref. 1, 2) A is a stable species or a free radical, B is a hydrogen atom or acetylene, and C is a free radical with the same number of carbon atoms as A, or a stable species with two more carbon atoms than A. In the ionic mechanism, A is an ion, B is acetylene, and C is an ion with two more carbon atoms than A.

The time for a single molecule, free radical or ion, per unit volume, to react is 1/R. Thus the time for any specific number of such species per unit volume to react is:

$$\tau = n/R. \tag{3}$$

where n is the number of such species reacting (for example the number of benzene molecules reacting) and R is the appropriate reaction rate for that step. We thus follow a specific number of soot precursor nuclei, n, as they move through the system, i.e., as they grow to larger species. By following these nuclei we measure the time it takes n of them to go from one step to the next, i.e., the time it takes to add a given number of carbon atoms.

For this exercise, we chose n as the maximum soot number density observed in this flame, 4×10^9 cm^{-3}. The number is not important for the comparison, but, as we will see, the use of the maximum number of soot particles has interesting implications.

The radical and ionic mechanisms for adding ten carbons to similarly sized species are given in Table 1. The time for each step is calculated by Eqs. (2) and (3) using the free radical rate coefficients from Frenklach et al. (ref. 1):

for A + H• (-H_2) $k = 1.7 \times 10^{-10}$ cm^3 s^{-1}

and for A + C_2H_2 (-H•) $k = 1.7 \times 10^{-11}$

and the ion-molecule reaction rate coefficient:

for A^+ + C_2H_2 (-D) $k = 1 \times 10^{-9}$.

In calculating the reaction times, only the forward reactions are considered for both mechanisms.

The total times required to add ten carbon atoms, Table 1, are comparable for the two mechanisms: 9.7 μs for the free radical mechanism and 5.6 μs for the ionic mechanism. The greater concentration of neutral species is balanced by the greater reaction rate coefficients for ion-molecule reactions and the fewer steps needed to add a specific number

FREE RADICAL MECHANISM

		Time, μs
$C_{10}H_8$		
↓ ↑ + H•	(- H_2)	0.27
$C_{10}H_7$•		
↓ + C_2H_2	(- H•)	0.11
$C_{12}H_8$		
↓ ↑ + H•	(- H_2)	0.64
$C_{12}H_7$•		
↓ ↑ + C_2H_2	(- H•)	0.16
$C_{14}H_8$		
↓ + H •	(- H_2)	2.7
$C_{14}H_7$•		
↓ + C_2H_2		1.1
$C_{16}H_9$•		
↓ ↑ cyclizes		
$C_{16}H_9$•		
↓ ↑ + C_2H_2	(- H•)	1.1
$C_{18}H_{10}$		
↓ + H •	(- H_2)	2.9
$C_{18}H_9$•		
↓ ↑ + C_2H_2	(- H•)	0.69
$C_{20}H_{10}$		
TOTAL TIME		9.7

IONIC MECHANISM

		Time, μs
$C_{11}H_9^+$		
↓ + C_2H_2	(-H_2)	3.1
$C_{13}H_9^+$		
↓ ↑ + C_2H_2		0.40
$C_{15}H_{11}^+$		
↓ + C_2H_2	(- H_2)	0.42
$C_{17}H_{11}^+$		
↓ + C_2H_2	(- H_2)	1.2
$C_{19}H_{11}^+$		
↓ + C_2H_2	(- H_2)	0.50
$C_{21}H_{11}^+$		
TOTAL TIME		5.6

TABLE 1

Comparison of the times required to add ten carbon atoms by the free radical and the ionic mechanisms

of carbon atoms to the growing species for the ionic mechanism than for the neutral mechanism.

Consideration of larger carbon containing species is not possible for the free radical mechanism because experimental data on large neutral species are not available in the standard flame, presumably because the concentrations are below detection limits. Delfau and Vovelle (ref. 16) give the flux of $C_{20}H_{12}$, but do not give the concentration; the mass flux for $C_{20}H_{12}$ is 1.4×10^{-5} compared with 4.6×10^{-5} for $C_{10}H_8$. From this, we estimate the concentration of $C_{20}H_{12}$ to be roughly an order of magnitude lower than that of $C_{10}H_8$:

benzene	C_6H_6	7.8×10^{12} cm^{-3}
naphthalene	$C_{10}H_8$	1.8×10^{11}
ethynylnaphthalene	$C_{12}H_8$	6.9×10^{10}
cyclopentacenaphthalene	$C_{14}H_8$	1.7×10^{10}
benzopyrene	$C_{20}H_{12}$	2×10^{10}

In the calculations of reaction times reported in Table 1, the neutral species concentrations for molecules larger than $C_{14}H_8$ had to be estimated from measurements in a different flame (ref. 18) because they were not available for the standard flame. Note above that there is a consistent decrease in the maximum concentration in going from C_6H_6 to $C_{14}H_8$ in the standard flame. This corresponds to roughly a three order of magnitude drop in concentration for an eight carbon atom increase in molecular size, and growth from one aromatic ring to four rings. The estimated value for the maximum concentration of $C_{20}H_{12}$ indicates a leveling off of this decay with size, an approximate order of magnitude concentration drop in adding ten carbons from $C_{10}H_8$ (two rings) to $C_{20}H_{12}$ (five rings). This is similar to the measurements of larger species by Bockhorn (ref. 18) in a different flame.

For ions, the overall decay in concentration with size is more gradual throughout the mass range of $C_3H_3^+$ to $C_{45}H_{17}^+$ (ref. 5), e.g.:

$C_3H_3^+$	4.7×10^8	cm^{-3}
$C_{30}H_{15}^+$	1.9×10^8	
$C_{45}H_{17}^+$	1.9×10^6	

Here there is an overall order of magnitude drop for each increase in ion size of 15 to 20 carbon atoms.

This comparison of growth times for the neutral and ionic mechanisms, using experimental species concentrations and typical rate coefficients used in the two respective mechanisms, demonstrates that the times to add ten carbon atoms, from C_{10} to C_{20}, by the two mechanisms are comparable. This analysis also demonstrates the need to go to larger species than C_{20} to determine the differences in the abilities of the two mechanisms to produce large carbon species.

We now consider the implications of the above calculations of reaction times. The maximum soot number density, Fig. 2, is reached at about 35 mm above the burner, or about 6.7 ms from the position in the flame at which large carbon containing species maximize. This is a good estimate of the time available, τ_s, for soot particles to be formed from molecular species. If we assume the time for the addition of one carbon atom to the growing species is τ_c, then the number of carbon atoms, N_c, that can be added to the growing nuclei is:

$$N_c = \frac{\tau_s}{\tau_c} = \frac{6.7 \times 10^{-3}}{7.4 \times 10^{-7}} \approx 9{,}000 \text{ carbon atoms.} \quad (4)$$

τ_c is taken as the average for the neutral and ion mechanisms, Table 1. 9,000 carbon atoms corresponds to a molecular weight of about 110,000 amu. This is equivalent to a particle diameter of about 4.5 or 3.0 nm, depending upon whether the particle is planar or spherical, respectively (ref. 3). The experimentally observed particle diameters at 35 mm above the burner surface are 9-13 nm for neutral particles and 3-6 nm for charged particles. It is

interesting that the calculated diameter, assuming the equivalent of a fixed rate (fixed time) for adding carbon atoms to the growing species, neutral or ion, leads to a diameter of the carbon particle very close to that observed, within the accuracy of the calculation and the measurement.

The main point of the above discussion is that examining relatively small carbon species does not permit a conclusion concerning the rate of soot nucleation by the neutral and the ionic mechanism; they both have about the same reaction times using the data that are available. To make a distinction between the two mechanisms one must examine reactions involving larger numbers of carbon atoms.

SUMMARY

An analysis of the well studied sooting acetylene-oxygen flame burning at 2.7 kPa indicates the following:

1. The total rate of ion formation and the net rate (total rate minus the rate of ion-electron recombination) are both greater than the rate of soot formation.

2. The location in the flame where ions disappear corresponds to the location where soot is formed.

3. The net rate of ion disappearance is approximately equal to the observed rate of soot formation if soot formation is taken to occur where the flame first becomes "yellow", and is about three times smaller if soot formation is taken where the soot particles are large enough to be observed in an electron microscope, about 1.5 nm.

4. For modest size carbon species, 10 to 20 carbon atoms, the rate of growth of carbon species is about the same for the neutral free radical mechanism and for the ionic mechanism. The greater concentration of neutral species is balanced by the greater reaction rate coefficients for ion-molecule reactions and the fewer number of steps involved in adding a specific number of carbon atoms to the growing species for the ionic mechanism than for the neutral mechanism.

5. The observed rates of growth of carbon species by the neutral or ionic mechanism are consistent with the maximum number density of soot observed in this flame.

6. Resolution of the question of whether soot particles are formed by a neutral free radical mechanism or by an ionic mechanism requires either the measurement of profiles in flames of larger neutral species or the calculation of such profiles by a reliable computer model.

7. Accurate concentration profile measurements of very small particles, bridging the gap between molecular and particulate systems, are desirable.

Acknowledgement

This research was sponsored by the US Air Force Office of Scientific Research (AFSC), under Contract F49620-88-C-0007. The United States Government is authorized to reproduce and distribute reprints for governmental purposes notwithstanding any copyright notation hereon. The authors are grateful to Drs. W. Felder and R. J. Gill for advice and criticism during the course of this work.

REFERENCES

1. M. Frenklach, and J. Warnatz, Combust. Sci. Techn. 51, 265 (1987).

2. M. Frenklach, D.W. Clary, W.G. Gardiner, Jr., and S.F. Stein, Twentieth Symposium (International) on Combustion, p. 887, The Combustion Institute, Pittsburgh (1984).

3. H.F. Calcote, Combust. Flame 42, 215 (1981).

4. D.G. Keil, R.J. Gill, D.B. Olson, and H.F. Calcote, Twentieth Symposium (International) on Combustion, p. 1129, The Combustion Institute, Pittsburgh (1985).

5. H.F. Calcote and D.G. Keil, Combust. Flame, 74, 131 (1988).

6. H.F. Calcote, D.B. Olson, and D.G. Keil, Energy & Fuels 2, 494 (1988).

7. A.N. Eraslan, and R.C. Brown, Combust. Flame 74, 191 (1988).

8. J.R. Eyler, The Chemistry of Combustion Processes, T.M. Sloane, Ed.; Advances in Chemistry Series No. 249, p.49, American Chemical Society, Washington, DC (1984).

9. K.C. Smyth, S.C. Lias, and P. Ausloos, Combust. Sci. Techn. 28, 147 (1982).

10. F. Ozturk, G. Baykut, M. Aoini, and J.R. Eyler, J. Phys. Chem. 91, 4360 (1987).

11. D. Smith and N.G. Adams, Int. J. Mass Spect. Ion Proc. 76, 307 (1987).

12. R. Patrick and D.M. Golden, J. Chem. Phys. 82, 75 (1985).

13. A. Cameron, J. Leszcyuski, M.C. Zerner, and B. Weiner, J. Phys. Chem. 93, 139 (1989).

14. P. Michaud, J.L. Delfau, and A. Barassin, Eighteenth Symposium (International) on Combustion, p. 443, The Combustion Institute, Pittsburgh (1981).

15. J.D. Bittner and J.B. Howard, Particulate Carbon: Formation During Combustion, D.G. Siegla and G.W. Smith, Eds., p. 109, Plenum, New York (1981).

16. J.L. Delfau and C. Vovelle, Combust. Sci. Techn. 41, 1 (1984).

17. J.B. Howard, B.L. Wersborg, and G.C. Williams, Faraday Symp. Chem. Soc. 7, 109 (1973).

18. H. Bockhorn, F. Fettig, and H.W. Wenz, Ber. Bunsenges. Phys. Chem. 87, 1067 (1983).